Received: 8 August 2021 | Revised: 29 September 2021 | Accepted: 31 October 2021

DOI: 10.1002/psp4.12746

ARTICLE

Physiologically-based pharmacokinetic modeling to predict CYP3A4-mediated drug-drug interactions of finerenone

Thomas Wendl[1] | **Sebastian Frechen**[1] | **Michael Gerisch**[2,3] | **Roland Heinig**[3] | **Thomas Eissing**[1]

[1]Pharmaceuticals R&D, Pharmacometrics, Bayer AG, Leverkusen, Germany

[2]Pharmaceuticals R&D, Drug Metabolism and Pharmacokinetics, Bayer AG, Wuppertal, Germany

[3]Pharmaceuticals R&D, Clinical Pharmacology, Bayer AG, Wuppertal, Germany

Correspondence
Thomas Eissing, Bayer AG, Pharmaceuticals R&D, Pharmacometrics, Building B106 Room 205, 51368 Leverkusen, Germany.
Email: thomas.eissing@bayer.com

Funding information
No funding was received for this work.

Abstract

Finerenone is a nonsteroidal, selective mineralocorticoid receptor antagonist that recently demonstrated its efficacy to delay chronic kidney disease (CKD) progression and reduce cardiovascular events in patients with CKD and type 2 diabetes. Here, we report the development of a physiologically-based pharmacokinetic (PBPK) model for finerenone and its application as a victim drug of cytochrome P450 3A4 (CYP3A4)-mediated drug-drug interactions (DDIs) using the open-source PBPK platform PK-Sim, which has recently been qualified for this application purpose. First, the PBPK model for finerenone was developed using physicochemical, in vitro, and clinical (including mass balance) data. Subsequently, the finerenone model was validated regarding the contribution of CYP3A4 metabolism to total clearance by comparing to observed data from dedicated clinical interaction studies with erythromycin (simulated geometric mean ratios of the area under the plasma concentration-time curve [AUCR] of 3.46 and geometric mean peak plasma concentration ratios [C_{max}Rs] of 2.00 vs. observed of 3.48 and 1.88, respectively) and verapamil (simulated AUCR of 2.91 and C_{max}R of 1.86 vs. observed of 2.70 and 2.22, respectively). Finally, the finerenone model was applied to predict clinically untested DDI studies with various CYP3A4 modulators. An AUCR of 6.31 and a C_{max}R of 2.37 was predicted with itraconazole, of 5.28 and 2.25 with clarithromycin, 1.59 and 1.40 with cimetidine, 1.57 and 1.38 with fluvoxamine, 0.19 and 0.32 with efavirenz, and 0.07 and 0.14 with rifampicin. This PBPK analysis provides a quantitative basis to guide the label and clinical use of finerenone with concomitant CYP3A4 modulators.

Study Highlights

WHAT IS THE CURRENT KNOWLEDGE ON THE TOPIC?

Kerendia (finerenone), a novel drug indicated in chronic kidney disease with type 2 diabetes, is a sensitive cytochrome P450 3A4 (CYP3A4) substrate. It was tested with the moderate CYP3A4 inhibitors erythromycin and verapamil in clinical

drug-drug interaction (DDI) studies influencing the pharmacokinetics (PKs) of finerenone.

WHAT QUESTION DID THIS STUDY ADDRESS?

What effects predict physiologically-based pharmacokinetics (PBPK) models for clinically untested CYP3A4 modulators on the finerenone PKs?

WHAT DOES THIS STUDY ADD TO OUR KNOWLEDGE?

This study complements the finerenone-drug interaction program informing scientists and prescribers as well as the drug label about the expected extent of CYP3A4 interactions on the finerenone PKs for inhibitors and inducers not tested clinically.

HOW MIGHT THIS CHANGE DRUG DISCOVERY, DEVELOPMENT, AND/OR THERAPEUTICS?

This PBPK model-based DDI assessment for finerenone applied a qualified CYP3A4 compound network approach using the open-source systems pharmacology platform (PK-Sim). As strong inhibitors and inducers were not studied clinically, such strong modulators did not provide the boundaries for interpolation to less sensitive DDI scenarios ("classical approach"), but were part of the prediction and thus extrapolated.

INTRODUCTION

Finerenone (Kerendia) is a nonsteroidal, selective mineralocorticoid receptor antagonist that recently demonstrated its efficacy to delay progression of kidney disease and to reduce the risk of cardiovascular events in patients with chronic kidney disease and type 2 diabetes in the pivotal outcome trial FIDELIO-DKD (ClinicalTrials.gov number, NCT02540993).[1]

The clinical pharmacology program for finerenone comprises 27 phase I studies to date and its main results have been published elsewhere.[2–7] The clinical program was complemented by population pharmacokinetic and pharmacodynamic (PopPKPD) analysis, including evaluations of patients in late-stage studies. PopPKPD analysis of the phase IIb studies ARTS-DN (NCT01874431) and ARTS-DN Japan (NCT01968668) have been published.[8–10]

The pharmacokinetics (PKs) of finerenone are dose-linear across the entire range of investigated doses (1.25 to 80 mg). Following oral administration, finerenone is rapidly and completely absorbed. It is eliminated almost exclusively by CYP3A4 metabolism and to a much smaller extent by CYP2C8.[2] Finerenone also shows a relevant first pass CYP3A4-mediated metabolism in both the gut wall and the liver. Based on clinical study data, the absolute bioavailability of finerenone after oral administration was 43.5%. A hepatic bioavailability of 0.756 and a fraction escaping gut wall metabolism (F_g) of 0.575 were calculated indicating that ~ 42% of orally administered finerenone was metabolized during first pass in the gut wall.[3] All formed major plasma metabolites are pharmacologically inactive. A small portion of finerenone (~ 1% of the dose) is renally eliminated unchanged by glomerular filtration. Plasma protein binding is moderate (about 92%).[3]

In the present study, a physiologically-based pharmacokinetic (PBPK) model for finerenone was developed and applied as a victim to predict CYP3A4-mediated drug-drug interactions (DDIs). For this purpose, the finerenone model was coupled to a set of various independently validated PBPK models of CYP3A4 modulators being part of a recently published CYP3A4-DDI compound network for the open-source PBPK platform PK-Sim, which has recently been qualified for this particular application purpose.[11–14] An overview of the interactions with finerenone discussed herein is shown in Figure 1.

The aim of the present modeling approach is to complement the clinical finerenone CYP3A4 DDI potential assessment, based on two dedicated clinical DDI studies with the mechanism-based inactivators (MBIs) erythromycin and verapamil, by PBPK.

METHODS

Finerenone PBPK model development

The PBPK model for finerenone was informed with physicochemical data (Table S1), clinical data including mass balance information (Table S2A[2]) and, in particular, data from the absolute bioavailability (BA) study (Table S2F[3]), the multiple dose escalation study (Table S2C) and a gemfibrozil DDI study (Table S2H). A complete list of clinical studies that were used for model development is shown in Table S2. The final PBPK model comprises metabolization

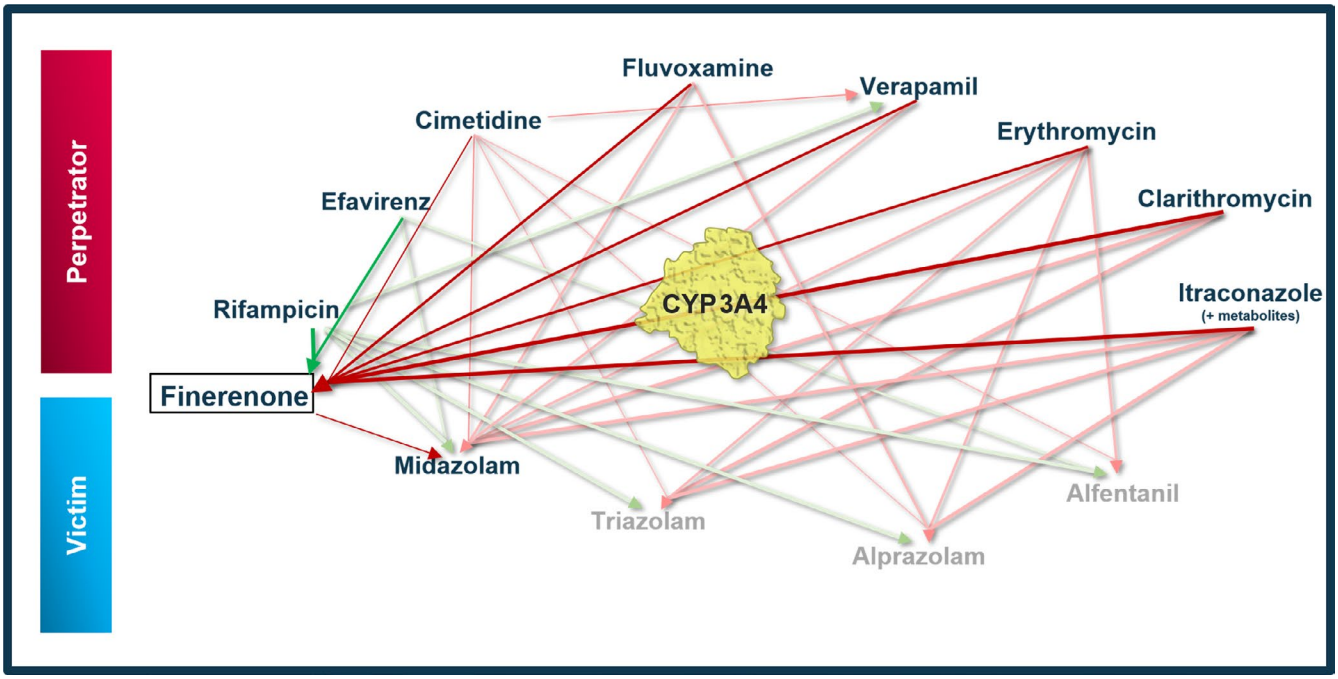

FIGURE 1 Simulated finerenone drug interactions (strong colors) with the established physiologically-based pharmacokinetic perpetrator models of the qualified network for CYP3A4-mediated DDI simulations (light colors). The arrows of the underlying CYP3A4 interaction network indicate where at least one clinical DDI study between the two connected substances was available and included in the model network. Red indicates inhibition and green indicates induction as the primary type of interaction. Thin arrows indicate weak, mid-thick arrows moderate and thick arrows strong CYP3A4 modulation by the perpetrator (figure modified from Frechen 2021). Please note that verapamil is exclusively a substrate in the combinations with rifampicin and cimetidine as, vice versa, rifampicin and cimetidine are not subject to CYP3A4 metabolism, and, hence, are not inhibited by verapamil. DDI, drug-drug interaction

via CYP3A4 and CYP2C8 and renal excretion of finerenone via glomerular filtration. A weak irreversible inhibition on CYP3A4 was observed in vitro[5] and, although negligible, it was included in the model by a mechanism-based CYP3A4 (auto-)inactivation (see below) as it may cooperate with CYP3A4 modulating processes of other perpetrators. The quantitative contribution of the CYP2C8 pathway was informed via an interaction study with the strong CYP2C8 inhibitor gemfibrozil. In this clinical study, an area under the plasma concentration-time curve ratio (AUCR) of 1.10 was observed for finerenone under gemfibrozil (600 mg twice daily [b.i.d.]) co-administration. Assuming complete inhibition of CYP2C8, the hepatic fm_{CYP3A4} was calculated to be $fm_{CYP3A4,hep} = 1/AUCR = 0.908$, and, consequentially, $fm_{CYP2C8,hep} = 1 - fm_{CYP3A4,hep} = 0.092$. The remaining hepatic metabolic clearance was assumed to be mediated solely by CYP3A4 and contributes to ~ 90% in the final model.

The parameter identification tool in PK-Sim has been used to estimate or optimize selected model parameters. These parameters (indicated in Table S1) were identified simultaneously using the complete training data set of Table S2 in a single parameter identification. Test and validation data sets were exclusively used for evaluation and excluded from parameter identification. Parameter correlation was assessed by checking the covariance matrix of parameter estimates. Most parameters were identified because they were either not determined (specific clearances, dissolution parameters, mucosa permeability on basolateral side, etc.) or determined with some uncertainties (CYP3A4 K_I and k_{inact}). Lipophilicity was adjusted as a surrogate parameter for partitioning as described in, for example, Kuepfer et al.[15] The extent of gut wall metabolization was estimated in the parameter identification using the parameter "mucosa permeability on basolateral side". This may lead to higher residence time in the enterocytes and, in turn, to a higher gut wall elimination. This parameter was preferred over other parameters, such as relative CYP3A4 expression or fraction unbound in the gut wall for technical reasons (not being limited to a maximum value). Additionally, the intrinsic clearances of CYP3A4 and CYP2C8 were estimated. Hereby, the contributions of CYP3A4 and CYP2C8 to total hepatic intrinsic clearance were informed via the hepatic fm_{CYP2C8}, as calculated above. Parameter identification was performed using a mean model approach with PK-Sim individuals reflecting weight and height of the mean individual of the corresponding clinical study.

Subsequently, the performance of the established finerenone model was evaluated in different settings, such

as acting as a CYP3A4 perpetrator in combination with midazolam, in a food effect study, and a high dose study. In this evaluation, data of two multiple dose studies (Table S2G) and two single dose studies (Table S2I,J) in healthy subjects were used.

The finerenone PK-Sim files are provided on https://github.com/Open-Systems-Pharmacology/Finerenone-Model.

Virtual populations

For the creation of the virtual phase I populations (i.e., one male population aged 18 to 45 years as well as populations according to an age- and gender study), demographic data of relevant clinical studies of finerenone were pooled and a multivariate distribution of age, body weight, and height was determined. The "PKSimCreatePopulation" algorithm, part of the OSP Matlab toolbox,[16] was supplied with this multivariate normal distribution and populations with 1000 individuals were created. This means that by design, the distribution of age, weight, and height of the virtual and the overall clinical study populations are comparable.

Validation of finerenone model as a CYP3A4 victim

The CYP3A4 contribution to the metabolic clearance of finerenone was validated using observed data from clinical DDI studies of finerenone with the moderate CYP3A4 inhibitors erythromycin (Table S2K) and verapamil (Table S2L). In these studies, finerenone co-administered with erythromycin (500 mg t.i.d.), classified as a moderate CYP3A4 inhibitor,[17] resulted in an AUCR and geometric mean peak plasma concentration ratio ($C_{max}R$) of 3.48 and 1.88, respectively. Verapamil (240 mg o.d.), also classified as moderate CYP3A4 inhibitor (and P-gp inhibitor), resulted in a finerenone AUCR and $C_{max}R$ of 2.70 and 2.22, respectively.

The established finerenone PBPK model was coupled to erythromycin and verapamil PBPK models that were validated independently as CYP3A4 perpetrator PBPK models.[11] Thereby, no parameters were modified or adjusted to simulate the virtual phase I population. The agreement between simulated and observed finerenone PKs under co-administration of erythromycin and verapamil, respectively, was assessed by a visual predictive check of the concentration-time profiles and comparing simulated versus observed AUCR and $C_{max}R$. The design of the simulations was chosen according to the clinical study design as described in Table S4.

Prediction of clinically untested DDI scenarios

After validation, the extent of interaction and the PKs of finerenone under co-administration of the CYP3A4 modulating perpetrator substances itraconazole, clarithromycin (both classified as strong index inhibitors), fluvoxamine (moderate inhibitor, classified as weak inhibitor until 2019), cimetidine (weak inhibitor), rifampicin (strong inducer), and efavirenz (moderate inducer, classification for all modulators on the US Food and Drug Administration [FDA] website on Drug Interactions, Tables of Substrates, Inhibitors, and Inducers)[18] was predicted through population simulations with the established virtual phase I population. For all treatments with CYP3A4 perpetrators, a control simulation with the same settings, but lacking perpetrator co-administration was performed to calculate AUCR and $C_{max}R$ (i.e., the ratios of the PK parameters of the victim drug [finerenone] under co-administration of a perpetrator over the control without co-administration).

For all perpetrator treatments, the maximum permissible dose was selected to reach the maximum inhibitory/inductive effect. Duration of treatment was selected using preliminary PBPK simulations to ensure that more than 95% of the maximum effect was reached. Administration of perpetrators was continued in the DDI model after finerenone administration to maintain the maximum effect. Finerenone was co-administered with typical offsets (e.g., 12 h after rifampicin dose to minimize the competitive inhibition of CYP3A4 by rifampicin), which may mask the effect of maximum induction.[13]

A list of perpetrators including simulated treatments is given in Table S4.

Sensitivity analysis

During model building (see above), the contributions of CYP3A4 and CYP2C8 to the hepatic metabolic clearance of finerenone were adjusted to ~ 0.9 (CYP3A4) versus 0.1 (CYP2C8). To evaluate the sensitivity of these hepatic fractions metabolized, the specific clearances of finerenone were adjusted to two scenarios yielding a hepatic fm_{CYP3A4} value of about 0.85 versus a hepatic fm_{CYP2C8} value of about 0.15 (scenario #1) and 0.95 versus 0.05 (scenario #2). For this purpose, specific clearances of CYP2C8 and CYP3A4 were re-adjusted before re-implementation into the PBPK model using the well-stirred model for the liver[19] and the Q_{gut} model[20] for gut wall metabolism to prevent deterioration of the overall model performance, in particular, to keep the total clearance and the fraction escaping F_g constant (see "Fraction metabolized adaption" in supplementary material).

Software, Open Systems Pharmacology PBPK model library, and platform qualification

The analysis was conducted using the software PK-Sim and MoBi as part of the Open Systems Pharmacology Suite (OSPS version 9.1.3, see www.open-systems-pharmacology.org) and Matlab (version R2017b). Perpetrator models were validated for the use in DDI simulations by the Open Systems Pharmacology community.[11] The qualification report can be found on OSP-Qualification-Reports,[21] the models are provided open source on the OSP PBPK Model Library.[22]

RESULTS

Finerenone PBPK model development and validation

Model parameters that were identified during the model building process are listed in Table S1. The estimated parameters were largely uncorrelated. Deviations of estimated to reference values—where applicable—were relatively small for most parameters.

Population simulations were performed using the final established PBPK model. A selection of simulated concentration-time profiles of the virtual phase I population in comparison to observed data is shown in Figure 2. The results show a good agreement of the simulated with the observed plasma-time concentration profiles over a variety of doses and dosing schedules, after intravenous or oral administration, and in different age and gender groups, overall, adequately reflecting the corresponding observed data and providing a quantitative understanding of the PKs.

The minor extent of mechanism-based CYP3A4 (auto-) inactivation in the finerenone PBPK model that was estimated within finerenone itself in the parameter identification is also reasonably describing the impact of finerenone on midazolam AUCR, as shown in Table S3. The established PBPK model overall describes diverse data from various phase I studies.

Validation of the finerenone PBPK model as a victim of CYP3A4-mediated drug interactions

The simulated AUCR of 3.46 with erythromycin (500 mg t.i.d.) is in line with the corresponding AUCR of 3.48 observed. In addition, the simulated $C_{max}R$ of 2.00 is in line with the $C_{max}R$ of 1.88 observed. Verapamil (120/240 mg o.d.) co-administration resulted in an AUCR of 2.91 in the simulation in line with the corresponding observed AUCR of 2.70. Moreover, the simulated $C_{max}R$ of 1.86 is comparable to the observed $C_{max}R$ of 2.22.[3] Thus, all presented simulated values fall within a range of 80–125% of the observed values. Additionally, the simulated variabilities of AUCR and $C_{max}R$ are comparable to the observed data for the effect of erythromycin or verapamil on finerenone.

Overall, the DDI model performance of the finerenone PBPK model as victim of CYP3A4-mediated interaction is regarded as accurate considering the good agreement between simulated and observed data (see Figure 3) and simulated and observed AUCRs and $C_{max}R$ (see Figure 4).

Prediction of clinically untested DDI scenarios with finerenone as victim of the DDI

The good performance in combination with the erythromycin and verapamil PBPK models adds confidence to the finerenone PBPK model, such that it can be considered validated for further extrapolations with the CYP3A4 modulators itraconazole, clarithromycin, fluvoxamine, cimetidine, rifampicin, and efavirenz.

A compilation of the predicted AUCR and $C_{max}R$ can be found in Figure 4.

Sensitivity analysis

Figure 5 confirms that the re-adjustment of the clearances in the two alternative scenarios shows the three investigated hepatic clearance proportions (i.e., 90% CYP3A4 and 10% CYP2C8 for the reference scenario, 85% CYP3A4 and 15% CYP2C8 for scenario #1, and 95% CYP3A4 and 5% CYP2C8 for scenario #2). Simulations of finerenone PKs after administration of different doses of finerenone show that the three scenarios are virtually indistinguishable confirming the similarity of the total clearance (systemic clearance and first pass metabolism) between the different scenarios (data not shown). The gemfibrozil interaction study was used to inform the finerenone model parameterization (see above). Correspondingly, the observed AUCR with gemfibrozil (1.10) is best described by the reference scenario (1.11), whereas scenario #1 slightly overpredicts (1.18) and scenario #2 slightly underpredicts (1.06) the observed data. A comparison of the three scenarios in DDI simulations with erythromycin (used for model validation, see above) demonstrates that the observed AUCR (3.48) is best described by the reference scenario (3.46), whereas scenario #1 (3.19) and scenario #2 (3.74) performed worse. Only in the case of verapamil (used for validation), the observed AUCR (2.70) was

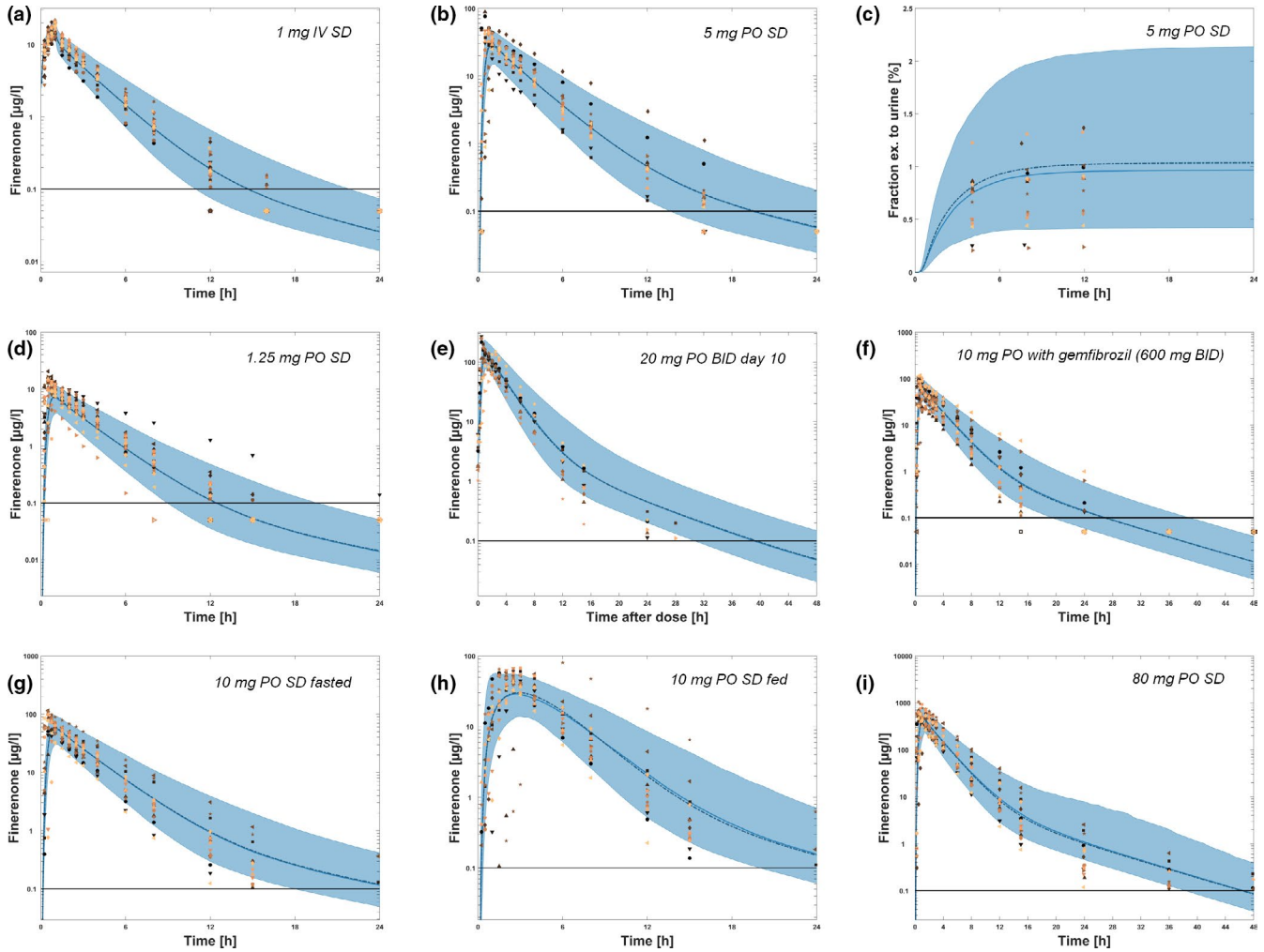

FIGURE 2 VPC of finerenone PK profiles for a representative subset of considered study arms. Time profiles show venous blood plasma concentrations on a logarithmic scale except in C where fraction excreted to urine is shown in linear scale. Clinical study IDs are found in Table S2. (a) 1 mg i.v. single dose (SD) from study F; (b) 5 mg peroral tablet (PO) SD from study F; (c) fraction excreted to urine of 5 mg p.o. SD from study F; (d) 1.25 mg tablet single dose from study E; (e) 20 mg (2 × 10 mg) tablet b.i.d. day 10 from study C; (f) 10 mg p.o. with gemfibrozil from study H; (g) 10 mg tablet SD fasted from study B; (h) 10 mg tablet SD fed from study B; (i) 80 mg (8 × 10 mg) tablet SD from study B. Blue area, simulated 5th and 95th percentile; blue solid line, simulated median; blue dashed line, simulated mean; symbols, observed data; black solid line, lower limit of quantification (LLOQ), in case observed data below LLOQ are available, they are displayed as LLOQ/2; IV, intravenous; PO, peroral tablet; SD, single dose; BID, twice daily. For all simulations, $n = 1000$

slightly better described by scenario #1 simulations (2.73) with the reference scenario performing second best (2.91). Table 1 summarizes AUCR and $C_{max}R$ of finerenone with the presented modulators in the different scenarios. Overall, the differences among the three scenarios are small and the reference scenario describes the evaluated interactions in a better way than scenarios #1 or #2.

DISCUSSION

A PBPK model was continuously developed to integrate and support the quantitative understanding of the PKs of finerenone. The model was developed based on preclinical data and data from several phase I studies. In the model building process, selected parameters were optimized to improve the fit to the observed study data.

Overall, the simulated PKs over a variety of doses and dosing schedules, as well as after intravenous (i.v.) and oral administration and different age and gender groups, adequately reflected the corresponding observed data. The variability of the observed data was also well captured by the model.

The contribution of CYP3A4 to finerenone total clearance could be validated as the coupled erythromycin- or verapamil-finerenone PBPK models show good agreement with the finerenone concentration-time profiles under co-administration of these perpetrators, as observed in

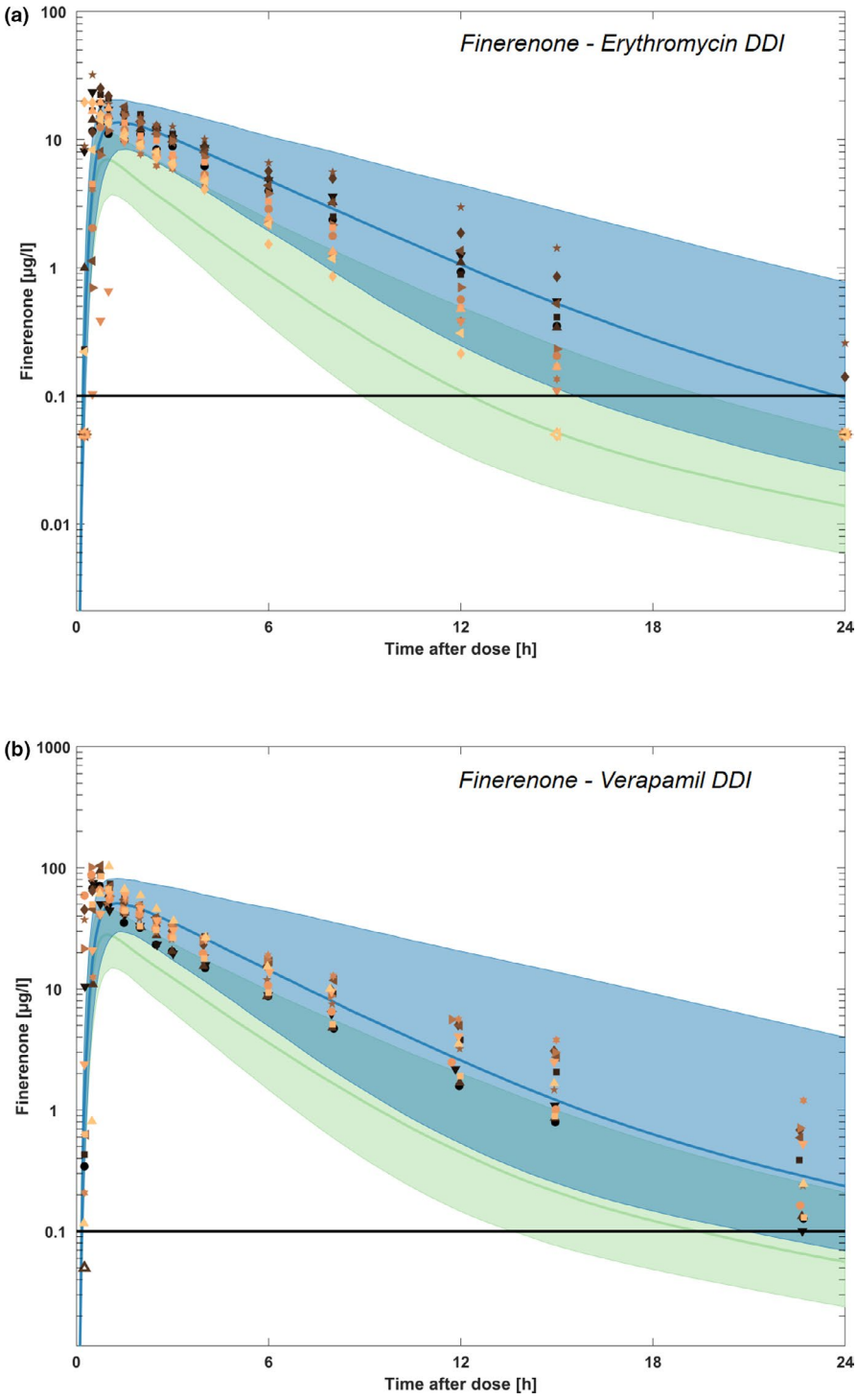

FIGURE 3 Finerenone (1.25 mg) and erythromycin (500 mg t.i.d.) co-administration (a); finerenone (5 mg) and verapamil (120/240 mg) co-administration (b) (see Table S4). (a) Finerenone concentration-time profiles under co-administration of erythromycin, blue solid line: simulated median for finerenone 1.25 mg and erythromycin 500 mg t.i.d.; green area: simulated 5th and 95th percentiles of time profiles of finerenone 1.25 mg control; green solid line: simulated median for finerenone 1.25 mg control. (b) Time profiles of finerenone under verapamil co-administration, blue solid line: simulated median for finerenone 5 mg and verapamil; green area: simulated 5th and 95th percentiles of time profiles of finerenone 5 mg control; green solid line: simulated median for finerenone 5 mg control; black solid line: lower limit of quantification (LLOQ), observed data below LLOQ are displayed as LLOQ/2. DDI, drug-drug interaction

clinical DDI studies. This enabled the use of the model to be applied in clinically untested scenarios.

In the fed state, the model slightly underestimates the observed data. Despite complete absorption in the fasted state, a small food effect was observed in clinical studies (10–21% AUC increase in fed state, studies B and J) that is not captured by the model. Here, other unknown factors that are not included in the model might explain this observation, however, the food effect is clinically not relevant as also indicated in the United States Prescribing Information (USPI) stating that finerenone tablets may be taken with or without food[23] and beyond the scope of the current model.

The mechanism-based auto-inactivation by finerenone occurs in both the liver and intestine, but, generally, its impact is low. Based on noncompartmental analysis (NCA) of multiple-dose studies where finerenone was administered at supratherapeutic doses (i.e., higher than labeled), the finerenone linearity factor R_{lin} (calculated as $AUC_{0-24,day10}/AUC_{inf,day1}$) was less than or equal to 1.32

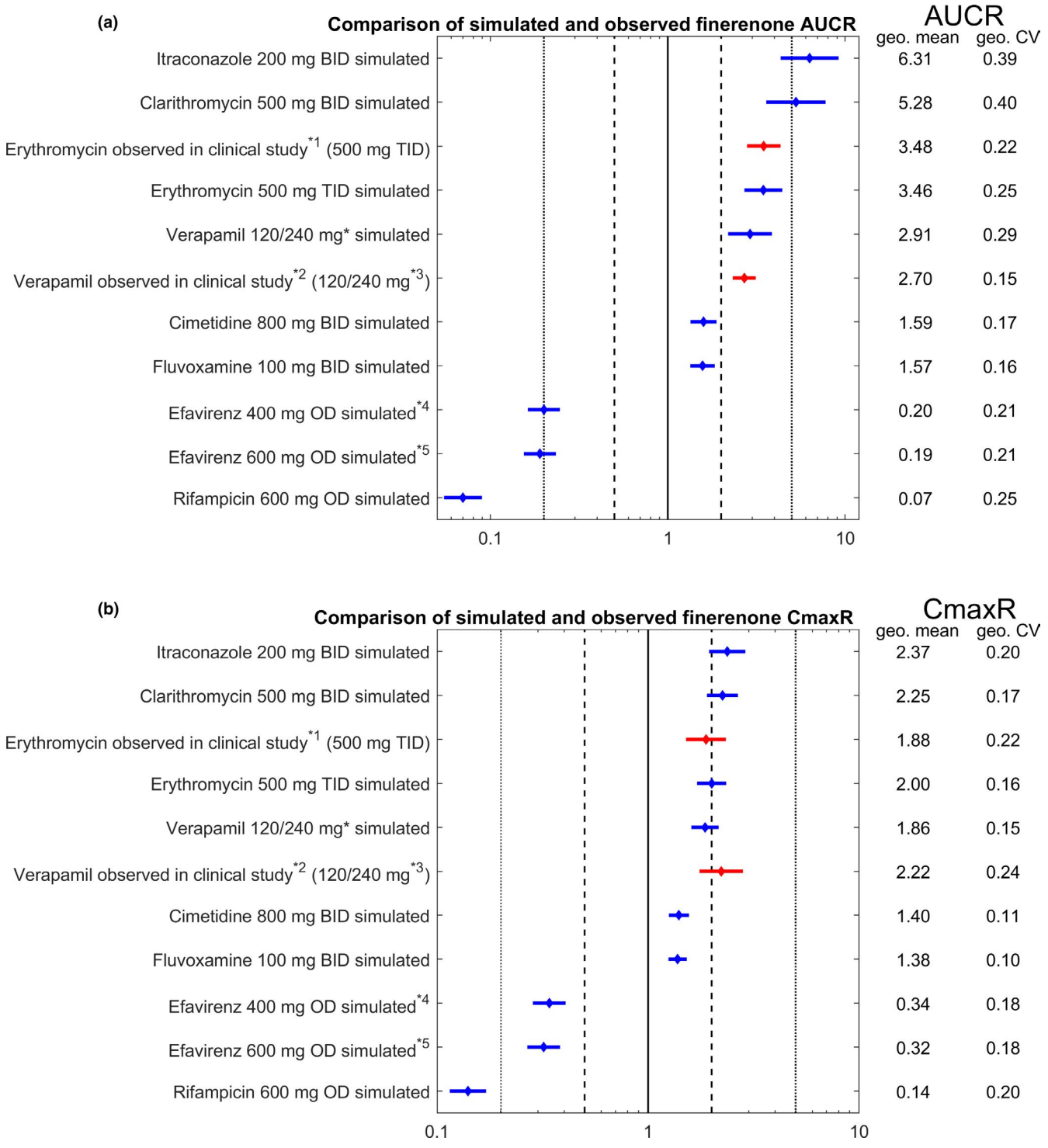

FIGURE 4 Simulated and observed finerenone AUCR (a) and $C_{max}R$ (b) and their variabilities in the order of decreasing AUCR values. Simulated ratios in blue, observed in red, solid line represents a ratio of one, dashed lines represent two-fold, dotted lines five-fold decrease/increase *1: see Table S2K, *2: see Table S2L, *3: Verapamil dosing see Table S4; *4: Frequently used dosing; *5: Maximum permissible dose leading to maximum effect. AUCR, area under the plasma concentration-time curve ratio; $C_{max}R$, peak plasma concentration ratio; OD, once daily; BID, twice a day; TID, three times a day

and the AUCR for midazolam was less than or equal to 1.21 (see Table S3). PBPK simulations for 10 mg finerenone once daily (OD) show that the effect is very small in the liver (i.e., a reduction in active CYP3A4 enzyme by ~ 0.4%), whereas a larger reduction by up to 40% is predicted in steady-state conditions in the intestine.

The predicted AUCR values of finerenone in combination with the perpetrator PBPK models of itraconazole,

TABLE 1 Comparison of observed and simulated AUCR and $C_{max}R$ and their CV for finerenone-drug interactions in different scenarios

Modulator	Scenario	AUCR geo. mean	AUCR geo. CV	$C_{max}R$ geo. mean	$C_{max}R$ geo. CV
Erythromycin	Observed in clinical study	3.48	0.22	1.88	0.22
	Simulated reference scenario	3.46	0.25	2.00	0.16
	Simulated scenario #1	3.19	0.25	1.93	0.16
	Simulated scenario #2	3.74	0.25	2.07	0.17
Verapamil	Observed in clinical study	2.70	0.15	2.22	0.24
	Simulated reference scenario	2.91	0.29	1.86	0.15
	Simulated scenario #1	2.73	0.28	1.80	0.15
	Simulated scenario #2	3.09	0.30	1.91	0.16
Gemfibrozil	Observed in clinical study	1.10	0.18	1.16	0.31
	Simulated reference scenario	1.11	0.08	1.06	0.04
	Simulated scenario #1	1.19	0.11	1.09	0.06
	Simulated scenario #2	1.06	0.04	1.03	0.02
Itraconazole	Simulated reference scenario	6.31	0.39	2.37	0.20
	Simulated scenario #1	5.23	0.39	2.24	0.19
	Simulated scenario #2	7.76	0.40	2.50	0.20
Clarithromycin	Simulated reference scenario	5.28	0.40	2.25	0.17
	Simulated scenario #1	4.52	0.38	2.14	0.16
	Simulated scenario #2	6.27	0.45	2.36	0.17
Fluvoxamine	Simulated reference scenario	1.57	0.16	1.38	0.10
	Simulated scenario #1	1.54	0.15	1.36	0.10
	Simulated scenario #2	1.59	0.16	1.39	0.10
Cimetidine	Simulated reference scenario	1.59	0.17	1.40	0.11
	Simulated scenario #1	1.56	0.17	1.39	0.11
	Simulated scenario #2	1.61	0.18	1.42	0.11
Efavirenz	Simulated reference scenario	0.19	0.21	0.32	0.18
	Simulated scenario #1	0.20	0.22	0.33	0.18
	Simulated scenario #2	0.18	0.21	0.31	0.18
Rifampicin	Simulated reference scenario	0.071	0.25	0.14	0.20
	Simulated scenario #1	0.074	0.26	0.15	0.21
	Simulated scenario #2	0.068	0.24	0.14	0.20

Abbreviations: AUCR, area under the plasma concentration-time curve ratio; $C_{max}R$, peak plasma concentration ratio; CV, coefficient of variation; geo., geometric.

clarithromycin, fluvoxamine, cimetidine, efavirenz, and rifampicin are closely in line with the published AUCR for sensitive CYP3A4 substrates like midazolam,[24–33] triazolam,[34,35] alprazolam,[36,37] or alfentanil[38–40] for comparable perpetrator dosing. Literature values for geometric mean (in some cases, arithmetic mean) AUCR of oral midazolam with multiple doses of 200 mg itraconazole range from 6.6 to 10.8,[24,30–32] or from 4.84 to 8.4 after multiple doses of 500 mg clarithromycin,[25,26,29,32] whereas AUCR was reported to be 1.66 for the fluvoxamine-midazolam interaction.[28] For rifampicin, mean AUC ratios between 0.0155 and 0.132 were observed.[24,41–44] Thus, the predicted values for the interaction with finerenone all fall within the published observed ranges for other victim drugs with comparable fractions metabolized via CYP3A4. In the case of fluvoxamine, currently classified as moderate CYP3A4 inhibitor,[18] the degree of inhibition of finerenone clearance supports the former classification as a weak CYP3A4 inhibitor.

In the case of induction by efavirenz, a mean AUCR value of 0.22 is reported for the effect of multiple doses of 600 mg efavirenz on the sensitive CYP3A4 substrate alfentanil.[40] This AUCR value is close to being classified as strong induction. Furthermore, midazolam PK under efavirenz co-administration as shown in, for example, Katzenmaier et al.,[45] suggest that AUCR might even be lower than 0.20. PBPK predictions of multiple doses of 600 mg efavirenz in combination with finerenone led to a

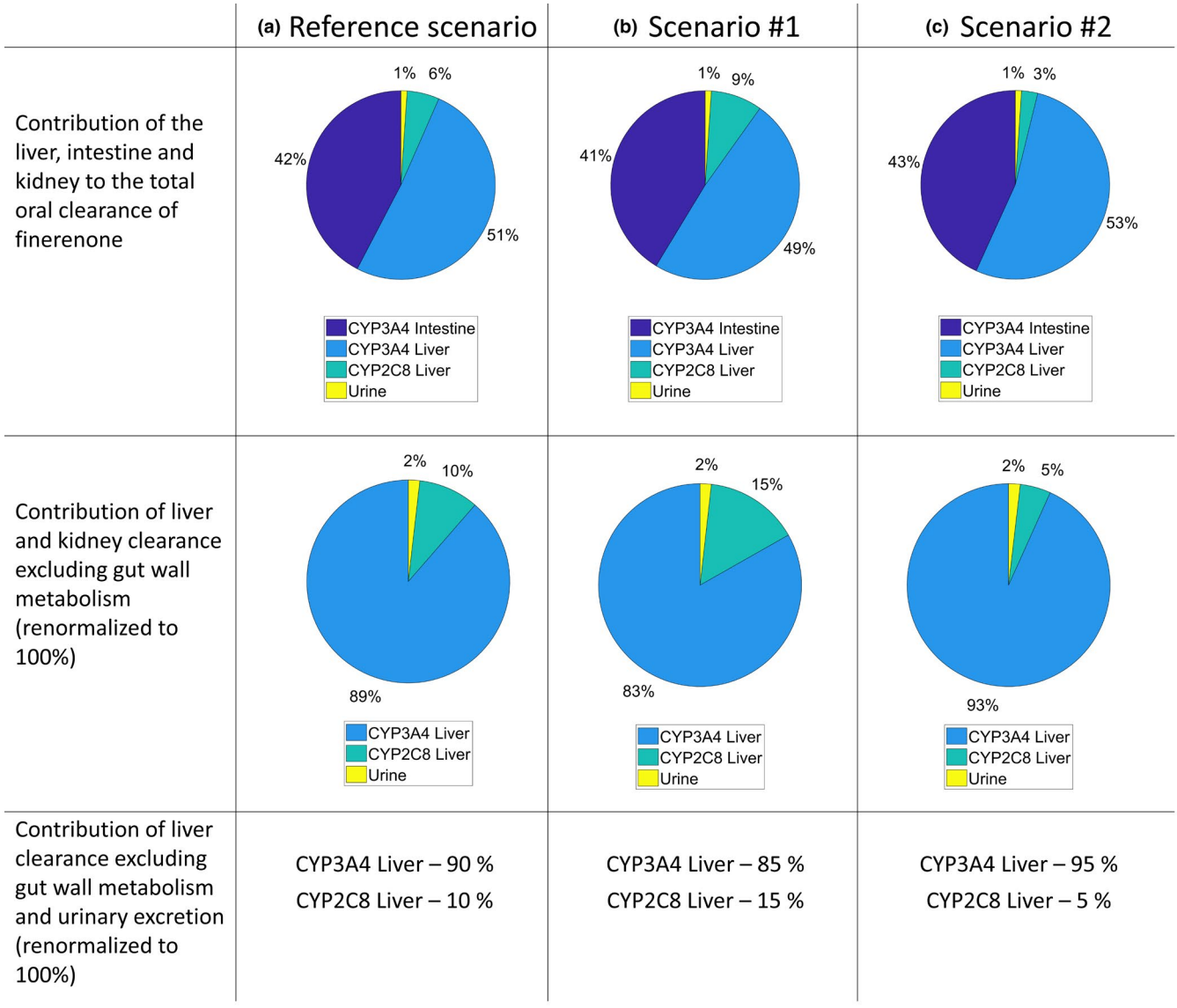

FIGURE 5 Model informed relative contribution of CYP3A4 and CYP2C8 calculated on the basis of the simulated 10 mg oral dose in the dose proportionality study (see Table S2E), (a) reference scenario, (b) scenario #1, (c) scenario #2

geometric mean AUCR of 0.19. This value is comparable to the observed value with alfentanil, nevertheless, this effect would be classified as strong based on the categories proposed by the FDA.[18] To elucidate the performance of the efavirenz PBPK model with respect to finerenone, an additional simulation with multiple doses of 400 mg efavirenz, a common clinical dosing, was performed. For multiple doses of 400 mg efavirenz, a geometric mean AUCR of slightly higher than 0.20 was predicted falling into the category of moderate induction.

Obviously, there is some uncertainty regarding the predicted strength of effect of the named perpetrators on finerenone. The geometric mean fold error (GMFE) of AUCR and $C_{max}R$ derived from the simulated combinations of the established DDI network on OSP can serve as a measure of mean uncertainty. For all simulated combinations of the CYP3A4-DDI network on OSP, it was calculated to be ~ 1.39 on AUC and 1.37 on C_{max}.[11] As a result of that, deviations in this range for all predictions may be expected. This can be broken down to the different types of mechanisms. For all included competitive inhibition simulations (i.e., the combinations with itraconazole, cimetidine, or fluvoxamine), the GMFE on AUCR was calculated to be 1.49, and 1.27 on $C_{max}R$. For all included MBI simulations (i.e., all combinations with clarithromycin, erythromycin, or verapamil), the GMFE on AUCR was calculated to be 1.27, and 1.24 on $C_{max}R$. For all included inducers (i.e., all combinations with efavirenz or rifampicin), the GMFE of AUCR was calculated to be 1.38, and 1.48 for $C_{max}R$.[21] For all these types of mechanisms, predictions with uncertainties in this range can be considered sufficiently accurate to inform the clinical use of finerenone with concomitant CYP3A4 modulators.

The PBPK simulated F_g of 0.5764 is an outcome of the parameter identification, in which the extent of gut wall metabolization was informed with PK data of the absolute bioavailability study (Table S2F), among others. The resulting finerenone model adequately describes PK data of the absolute bioavailability study after i.v. and oral administration (see Figure 2a,b), hence, F_g and bioavailability should be adequately captured. Furthermore, the PBPK simulated F_g is almost identical to the previously published F_g of 0.575 based on NCA of the absolute BA study.[3]

The total fm_{CYP3A4} (of total oral clearance) in the finerenone PBPK model is ~ 0.93, which is composed of 0.42 in the gut wall and 0.51 in the liver (see Figure 5a). This can be considered as an upper boundary because of the assumption in the model-building process in which the clearance contribution in the PBPK model was informed with the clinically observed AUCR of the gemfibrozil interaction study. Here, it was assumed that gemfibrozil inhibits CYP2C8 by 100% such that the resulting total fm_{CYP2C8} of ~ 0.05 can be considered as lower boundary. The remaining metabolic clearance was then assumed to be exclusively mediated via CYP3A4, and, hence, is an upper boundary.

This is fully in line with fm_{CYP3A4} estimations reported by Heinig et al.[3] who performed static model calculations that are based on the equations published by Ohno et al.[46] and Loue and Tod[47] and reported point estimates for fm_{CYP3A4} being 0.88 and 0.89 for calculations based on erythromycin and verapamil data, respectively. Taking uncertainty in the underlying clinical interaction studies into account and propagating the reported 90% confidence intervals of the AUCR (i.e., [3.017; 4.019] for erythromycin and [2.4295; 3.0082] for verapamil), this would translate to a fm_{CYP3A4} range of 0.83 to 0.94.

In PBPK modeling practice, extrapolation of DDI is often made from strong perpetrators to moderate or weak perpetrators. In this study, it was the other way around. Therefore, a sensitivity analysis was performed on fm_{CYP3A4} to evaluate the uncertainty regarding the DDI potential of finerenone with strong inhibitors and moderate or strong inducers. This sensitivity analysis shows that the differences among the three scenarios are small and the reference scenario with the parameters as obtained in the parameter identification describes the evaluated interactions in a better way than the other investigated scenarios with slightly higher or lower fm_{CYP3A4}. To address the impact of uncertainty in DDI extrapolations, the investigated alterations of fm_{CYP3A4} were propagated to all predictions providing ranges for expected interactions, as displayed in Table 1. This is considered especially important when extrapolating DDI effects to stronger modulators than tested clinically.

Generally, DDIs that increase or decrease drug exposure can influence the benefit risk assessment of a drug and can impose a safety risk or attenuate efficacy, respectively, and should be considered in recommendations on drug use. Regarding efficacy, finerenone was shown to significantly reduce the primary albuminuria end point (UACR; urinary albumin to creatinine ratio) at dose levels as low as 7.5 mg OD in the phase IIb study ARTS-DN.[9] PopPKPD analysis indicated that effects on the efficacy marker UACR as well as the safety markers serum potassium and acute estimated glomerular filtration rate (eGFR) decline were saturating towards the highest tested dose of 20 mg OD overall revealing non-steep exposure-response relationships.[8] In the pivotal phase III study, FIDELIO-DKD, finerenone demonstrated efficacy and safety in a titration scheme, where 10 mg or 20 mg finerenone OD were administered based on serum potassium and eGFR.[1] On grounds of FIDELIO-DKD, finerenone was recently approved by the FDA with dosing guidance for clinical practice, including monitoring and dose adjustment rules. PopPKPD analyses of FIDELIO-DKD further supported the general benefit-risk assessment and the labeled wording on dosage and administration.[23,48,49] In particular, they highlighted and explained the role of serum potassium-based dose titration, inverting the observed dose-exposure-response relationship for serum potassium, as important context for CYP3A4 inhibitor label guidance.[23,48] Strong CYP3A4 inhibitors are contraindicated. For moderate or weak CYP3A4 inhibitors, it is recommended to monitor serum potassium during drug initiation or dosage adjustment of either finerenone or the CYP3A4 inhibitor, and adjust finerenone dosage as appropriate. Concomitant use of strong or moderate CYP3A4 inducers should be avoided.

The presented PBPK analyses of finerenone as victim of CYP3A4-mediated DDI can be considered in lieu of clinical DDI study-based data for modulator categories lacking such studies and contribute to the overall DDI assessment as reflected, for example, in the USPI under "Drug Interaction Studies - Clinical Studies and Model-Informed Approaches."[23]

ACKNOWLEDGEMENTS

The authors thank the OSP community, Sulav Duwal for Matlab support, Andreas Seelmann for preparing the clinical study data, Simone Steinbach for medical writing support, and Wolfgang Mueck for adding motivation to the conduct of the PBPK DDI assessment.

CONFLICT OF INTEREST

T.W., S.F., M.G., R.H., and T.E. are Bayer employees and potential shareholders of Bayer AG. T.W. and S.F. use Open Systems Pharmacology software, tools, or models in their professional roles. S.F. is a member of the Open-Systems-Pharmacology Sounding Board.

AUTHOR CONTRIBUTIONS

T.W. and T.E. wrote the manuscript. T.W., S.F., M.G., R.H., and T.E., designed the research. T.W. and S.F. performed the research. T.W. and T.E. analyzed the data.

ORCID

Thomas Wendl https://orcid.org/0000-0002-1153-7167
Sebastian Frechen https://orcid.org/0000-0003-1170-9392
Michael Gerisch https://orcid.org/0000-0003-3807-9036
Roland Heinig https://orcid.org/0000-0002-4645-5428
Thomas Eissing https://orcid.org/0000-0003-4378-3423

REFERENCES

1. Bakris GL, Agarwal R, Anker SD, et al. Effect of finerenone on chronic kidney disease outcomes in type 2 diabetes. *N Engl J Med*. 2020;383(23):2219-2229.
2. Gerisch M, Heinig R, Engelen A, et al. Biotransformation of finerenone, a novel nonsteroidal mineralocorticoid receptor antagonist, in dogs, rats, and humans, in vivo and in vitro. *Drug Metab Dispos*. 2018;46(11):1546-1555.
3. Heinig R, Gerisch M, Engelen A, Nagelschmitz J, Loewen S. Pharmacokinetics of the novel, selective, non-steroidal mineralocorticoid receptor antagonist finerenone in healthy volunteers: results from an absolute bioavailability study and drug-drug interaction studies in vitro and in vivo. *Eur J Drug Metab Pharmacokinet*. 2018;43(6):715-727.
4. Heinig R, Lambelet M, Nagelschmitz J, Alatrach A, Halabi A. Pharmacokinetics of the novel nonsteroidal mineralocorticoid receptor antagonist finerenone (BAY 94–8862) in individuals with mild or moderate hepatic impairment. *Eur J Drug Metab Pharmacokinet*. 2019;44(5):619-628.
5. Heinig R, Gerisch M, Bairlein M, Nagelschmitz J, Loewen S. Results from drug-drug interaction studies in vitro and in vivo investigating the effect of finerenone on the pharmacokinetics of comedications. *Eur J Drug Metab Pharmacokinet*. 2020;45(4):433-444.
6. Lentini S, Heinig R, Kimmeskamp-Kirschbaum N, Wensing G. Pharmacokinetics, safety and tolerability of the novel, selective mineralocorticoid receptor antagonist finerenone - results from first-in-man and relative bioavailability studies. *Fundam Clin Pharmacol*. 2016;30(2):172-184.
7. Heinig R, Kimmeskamp-Kirschbaum N, Halabi A, Lentini S. Pharmacokinetics of the novel nonsteroidal mineralocorticoid receptor antagonist finerenone (BAY 94–8862) in individuals with renal impairment. *Clin Pharmacol Drug Develop*. 2016;5(6):488-501.
8. Snelder N, Heinig R, Drenth HJ, et al. Population pharmacokinetic and exposure-response analysis of finerenone: insights based on phase IIb data and simulations to support dose selection for pivotal trials in type 2 diabetes with chronic kidney disease. *Clin Pharmacokinet*. 2020;59(3):359-370.
9. Bakris GL, Agarwal R, Chan JC, et al. Effect of finerenone on albuminuria in patients with diabetic nephropathy: a randomized clinical trial. *JAMA*. 2015;314(9):884-894.
10. Bakris GL, Nowack C. Finerenone for albuminuria in patients with diabetic nephropathy-reply. *JAMA*. 2016;315(3):306.
11. Frechen S, Solodenko J, Wendl T, et al. A generic framework for the PBPK platform qualification of PK-sim and its application to predicting CYP3A4-mediated drug-drug interactions. *CPT Pharmacomet Syst Pharmacol* 2021;10(6):633-644.
12. Britz H, Hanke N, Volz AK, et al. Physiologically-based pharmacokinetic models for CYP1A2 drug-drug interaction prediction: a modeling network of fluvoxamine, theophylline, caffeine, rifampicin, and midazolam. *CPT Pharmacomet Syst Pharmacol*. 2019;8(5):296-307.
13. Hanke N, Frechen S, Moj D, et al. PBPK models for CYP3A4 and P-gp DDI prediction: a modeling network of rifampicin, itraconazole, clarithromycin, midazolam, alfentanil, and digoxin. *CPT Pharmacomet Syst Pharmacol*. 2018;7(10):647-659.
14. Türk D, Hanke N, Wolf S, et al. Physiologically based pharmacokinetic models for prediction of complex CYP2C8 and OATP1B1 (SLCO1B1) drug–drug–gene interactions: a modeling network of gemfibrozil, repaglinide, pioglitazone, rifampicin, clarithromycin and itraconazole. *Clin Pharmacokinet*. 2019;58(12):1595-1607.
15. Kuepfer L, Niederalt C, Wendl T, et al. Applied concepts in PBPK modeling: how to build a PBPK/PD model. *CPT Pharmacomet Syst Pharmacol*. 2016;5(10):516-531.
16. OSP. Opens Systems Pharmacology | Matlab-Toolbox v8.0.10. 2021 [cited June 29, 2021]. Available from: https://github.com/Open-Systems-Pharmacology/Matlab-Toolbox-Core/tree/970fcd890cc563c0656d605b092aa3da682959a3/code/auxiliaries.
17. FDA. Drug Development and Drug Interactions | Table of Substrates, Inhibitors and Inducers. 2021 [cited June 29, 2021]. Available from: https://www.fda.gov/drugs/drug-interactions-labeling/drug-development-and-drug-interactions-table-substrates-inhibitors-and-inducers.
18. FDA. Drug Development and Drug Interactions: Table of Substrates, Inhibitors and Inducers. 2020 [cited May 10, 2021]. Available from: https://www.fda.gov/drugs/drug-interactions-labeling/drug-development-and-drug-interactions-table-substrates-inhibitors-and-inducers%inVivo.
19. Yang J, Jamei M, Yeo KR, Rostami-Hodjegan A, Tucker GT. Misuse of the well-stirred model of hepatic drug clearance. *Drug Metab Disposit Biol Fate Chem*. 2007;35(3):501-502.
20. Yang J, Jamei M, Yeo KR, Tucker GT, Rostami-Hodjegan A. Prediction of intestinal first-pass drug metabolism. *Curr Drug Metab*. 2007;8(7):676-684.
21. OSP. Open Systems Pharmacology | CYP3A4 DDI Qualification Report v9.1.1. 2021 [cited June 29, 2021]. Available from: https://github.com/Open-Systems-Pharmacology/OSP-Qualification-Reports/blob/v9.1.1/DDI_Qualification_CYP3A4/report.md.
22. OSP. Open Systems Pharmacology | PBPK Model Library v9.1.1. 2021 [cited June 29, 2021] Available from: https://github.com/Open-Systems-Pharmacology/OSP-PBPK-Model-Library/tree/v9.1.1.
23. FDA. Kerendia (finerenone) US Prescribing Information 2021 [cited July 16, 2021]. Available from: www.accessdata.fda.gov/drugsatfda_docs/label/2021/215341s000lbl.pdf.
24. Backman JT, Kivistö KT, Olkkola KT, Neuvonen PJ. The area under the plasma concentration-time curve for oral midazolam is 400-fold larger during treatment with itraconazole than with rifampicin. *Eur J Clin Pharmacol*. 1998;54(1):53-58.
25. Gorski JC, Jones DR, Haehner-Daniels BD, Hamman MA, O'Mara EM Jr, Hall SD. The contribution of intestinal and hepatic CYP3A to the interaction between midazolam and clarithromycin. *Clin Pharmacol Ther*. 1998;64(2):133-143.

26. Gurley B, Hubbard MA, Williams DK, et al. Assessing the clinical significance of botanical supplementation on human cytochrome P450 3A activity: comparison of a milk thistle and black cohosh product to rifampin and clarithromycin. *J Clin Pharmacol*. 2006;46(2):201-213.
27. Gurley BJ, Swain A, Hubbard MA, et al. Supplementation with goldenseal (Hydrastis canadensis), but not kava kava (Piper methysticum), inhibits human CYP3A activity in vivo. *Clin Pharmacol Ther*. 2008;83(1):61-69.
28. Lam YW, Alfaro CL, Ereshefsky L, Miller M. Pharmacokinetic and pharmacodynamic interactions of oral midazolam with ketoconazole, fluoxetine, fluvoxamine, and nefazodone. *J Clin Pharmacol*. 2003;43(11):1274-1282.
29. Markert C, Hellwig R, Burhenne J, et al. Interaction of ambrisentan with clarithromycin and its modulation by polymorphic SLCO1B1. *Eur J Clin Pharmacol*. 2013;69(10):1785-1793.
30. Olkkola KT, Ahonen J, Neuvonen PJ. The effects of the systemic antimycotics, itraconazole and fluconazole, on the pharmacokinetics and pharmacodynamics of intravenous and oral midazolam. *Anest Analg*. 1996;82(3):511-516.
31. Olkkola KT, Backman JT, Neuvonen PJ. Midazolam should be avoided in patients receiving the systemic antimycotics ketoconazole or itraconazole. *Clin Pharmacol Ther*. 1994;55(5):481-485.
32. Prueksaritanont T, Tatosian DA, Chu X, et al. Validation of a microdose probe drug cocktail for clinical drug interaction assessments for drug transporters and CYP3A. *Clin Pharmacol Ther*. 2017;101(4):519-530.
33. Quinney SK, Haehner BD, Rhoades MB, Lin Z, Gorski JC, Hall SD. Interaction between midazolam and clarithromycin in the elderly. *Br J Clin Pharmacol*. 2008;65(1):98-109.
34. Greenblatt DJ, von Moltke LL, Harmatz JS, et al. Inhibition of triazolam clearance by macrolide antimicrobial agents: in vitro correlates and dynamic consequences. *Clin Pharmacol Ther*. 1998;64(3):278-285.
35. Villikka K, Kivistö KT, Backman JT, Olkkola KT, Neuvonen PJ. Triazolam is ineffective in patients taking rifampin. *Clin Pharmacol Ther*. 1997;61(1):8-14.
36. Fleishaker JC, Hulst LK. A pharmacokinetic and pharmacodynamic evaluation of the combined administration of alprazolam and fluvoxamine. *Eur J Clin Pharmacol*. 1994;46(1):35-39.
37. Schmider J, Brockmöller J, Arold G, Bauer S, Roots I. Simultaneous assessment of CYP3A4 and CYP1A2 activity in vivo with alprazolam and caffeine. *Pharmacogenetics*. 1999;9(6):725-734.
38. Kharasch ED, Vangveravong S, Buck N, et al. Concurrent assessment of hepatic and intestinal cytochrome P450 3A activities using deuterated alfentanil. *Clin Pharmacol Ther*. 2011;89(4):562-570.
39. Kharasch ED, Walker A, Hoffer C, Sheffels P. Intravenous and oral alfentanil as in vivo probes for hepatic and first-pass cytochrome P450 3A activity: noninvasive assessment by use of pupillary miosis. *Clin Pharmacol Ther*. 2004;76(5):452-466.
40. Kharasch ED, Whittington D, Ensign D, et al. Mechanism of efavirenz influence on methadone pharmacokinetics and pharmacodynamics. *Clin Pharmacol Ther*. 2012;91(4):673-684.
41. Backman JT, Olkkola KT, Neuvonen PJ. Rifampin drastically reduces plasma concentrations and effects of oral midazolam. *Clin Pharmacol Ther*. 1996;59(1):7-13.
42. Chung E, Nafziger AN, Kazierad DJ, Bertino JS Jr. Comparison of midazolam and simvastatin as cytochrome P450 3A probes. *Clin Pharmacol Ther*. 2006;79(4):350-361.
43. Link B, Haschke M, Grignaschi N, et al. Pharmacokinetics of intravenous and oral midazolam in plasma and saliva in humans: usefulness of saliva as matrix for CYP3A phenotyping. *Br J Clin Pharmacol*. 2008;66(4):473-484.
44. Reitman ML, Chu X, Cai X, et al. Rifampin's acute inhibitory and chronic inductive drug interactions: experimental and model-based approaches to drug-drug interaction trial design. *Clin Pharmacol Ther*. 2011;89(2):234-242.
45. Katzenmaier S, Markert C, Mikus G. Proposal of a new limited sampling strategy to predict CYP3A activity using a partial AUC of midazolam. *Eur J Clin Pharmacol*. 2010;66(11):1137-1141.
46. Ohno Y, Hisaka A, Suzuki H. General framework for the quantitative prediction of CYP3A4-mediated oral drug interactions based on the AUC increase by coadministration of standard drugs. *Clin Pharmacokinet*. 2007;46(8):681-696.
47. Loue C, Tod M. Reliability and extension of quantitative prediction of CYP3A4-mediated drug interactions based on clinical data. *AAPS J*. 2014;16(6):1309-1320.
48. Goulooze B, Snelder N, Seelmann A, et al. Finerenone dose-exposure-serum potassium response analysis of FIDELIO-DKD phase 3 - The role of dosing, titration, and inclusion criteria. Clin Pharmacokinet. 10.1007/s40262-021-01083-1
49. van den Berg P, Ruppert M, Mesic E, et al. Finerenone dose-exposure-primary efficacy response in FIDELIO-DKD phase 3 – Population pharmacokinetic and time-to-event analysis. Clin Pharmacokinet. 10.1007/s40262-021-01082-2

SUPPORTING INFORMATION

Additional supporting information may be found in the online version of the article at the publisher's website.

How to cite this article: Wendl T, Frechen S, Gerisch M, Heinig R, Eissing T. Physiologically-based pharmacokinetic modeling to predict CYP3A4-mediated drug-drug interactions of finerenone. *CPT Pharmacometrics Syst Pharmacol*. 2022;11:199–211. doi:10.1002/psp4.12746